



# Studies on *n*- and *p*-type metal oxide compounds for thermoelectric device fabrication

APOORVA P JOSHI<sup>1</sup>, S BHATTACHARYA<sup>2</sup> and S RAYAPROL<sup>3,\*</sup>

<sup>1</sup>Sri Jaychamrajendra College of Engineering, Mysuru 570006, India

<sup>2</sup>Technical Physics Division, Bhabha Atomic Research Centre, Mumbai 400085, India

<sup>3</sup>UGC-DAE Consortium for Scientific Research, Mumbai Centre, BARC Campus, Trombay, Mumbai 400085, India

\*Author for correspondence (suhindra@csr.res.in)

MS received 20 January 2017; accepted 2 May 2017; published online 5 February 2018

**Abstract.** We report the high-temperature thermoelectric properties of electron- and hole-doped calcium manganese oxide materials, which exhibit potential of a thermoelectric device for conversion of wasteful thermal energy into useful electrical energy. Electron-doped  $\text{Ca}_{0.9}\text{R}_{0.1}\text{MnO}_3$  ( $\text{R} = \text{La}, \text{Yb}$ ) and hole-doped  $\text{Ca}_4\text{Mn}_{2.85}\text{Nb}_{0.15}\text{O}_{10}$  manganites chosen for the present study were prepared by solid-state reaction of starting compounds and characterized by powder X-ray diffraction. Electrical resistivity and thermopower were measured as a function of temperature to determine the power factor for all the three compounds studied. We discuss these results according to their application potential as a thermoelectric device.

**Keywords.** Thermoelectric; X-ray diffraction; manganites.

## 1. Introduction

Nowadays, there is tremendous interest among scientists and engineers in developing newer materials and sources for energy harvesting [1]. Among these renewable energy sources, thermoelectric materials are gaining considerable attention as they can be useful in converting the wasteful heat energy, such as direct solar energy, excess heat from the car engines, etc. into productive electrical energy [2–5]. Thermoelectric materials work on the principles of Seebeck effect and Peltier effect [5]. Electric current flows when two dissimilar charge carrying semiconductors that are *n*-type and *p*-type materials connected in series and are subjected to a thermal gradient, which is shown as a schematic diagram in figure 1.

From applications point of view, the material which exhibits high efficiency in converting heat into electricity is highly desirable. This is quantified by a dimensionless quantity known as the thermoelectric figure of merit, given as  $ZT = S^2\sigma/\kappa$  [5]. The  $ZT$  is derived from the Seebeck coefficient ( $S$ ), electrical conductivity ( $\sigma$ ) and the total thermal conductivity ( $\kappa$ ) of the material, which is taken for the study and  $T$  is the absolute temperature.

There are several thermoelectric materials reported in the literature with  $ZT \sim 1$ , such as  $\text{AgSbTe}_2$ ,  $\text{PbTe}$ ,  $\text{SnTe}$ ,  $\text{SiGe}$ , etc. Recently, there were some interesting reports where  $ZT > 1$  was reported for similar compounds [6–8]. However, their applicability is not feasible till now due to various reasons, such as limited range of temperatures, difficulty in preparing materials in large quantities, toxicity of elements, degradation as a function of time or temperature, etc.

In such a situation, there is a need for environmentally safe efficient thermoelectric materials, which offer wider temperature range of operation, and are stable as a function of time and temperature variations. In the present work, we have made an attempt to identify oxide-based ceramic semiconductors for their thermoelectric properties and their potential application as thermoelectric generators, by choosing appropriate *n*-type and *p*-type semiconductors. It is well known in the literature that for high  $ZT$ , the resistivity ( $\rho$ ) and thermal conductivity ( $\kappa$ ) should be kept minimal. But with decreasing resistivity, thermal conductivity increases. Thermal conductivity can be reduced by the scattering of phonons on various types of defects, including the boundaries of any crystal. Ioffe *et al* [9] suggested that by forming a solid solution between two semiconductors that have the same crystal structure should lead to a reduction in the lattice conductivity.

Keeping these criteria in mind, we choose one *n*-type semiconductor,  $\text{Ca}_4\text{Mn}_{2.85}\text{Nb}_{0.15}\text{O}_{10}$  [10,11], and two *p*-type semiconductors,  $\text{Ca}_{0.9}\text{R}_{0.1}\text{MnO}_3$  ( $\text{R} = \text{La}, \text{Yb}$ ) [9] for comparing their electrical power factor ( $S^2/\rho$ ), which gives a fair idea about their functionality as elements of a thermoelectric generator.

## 2. Experimental

All the three samples studied during the course of this work were prepared by the solid-state reaction of the starting compounds. Stoichiometric quantities of  $\text{CaCO}_3$ ,  $\text{MnO}_2$ ,  $\text{Nb}_2\text{O}_5$ ,  $\text{La}_2\text{O}_3$  and  $\text{Yb}_2\text{O}_3$  (all with stated purities better than 99.9%)

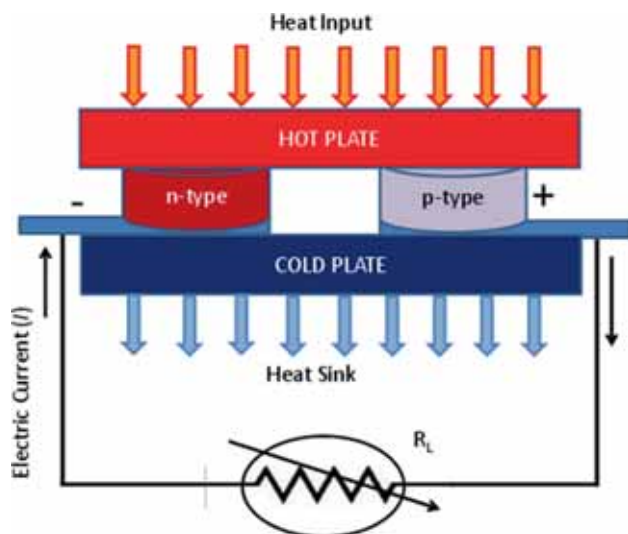


**Figure 1.** Schematics of a thermoelectric generator.

were taken for preparing  $\text{Ca}_4\text{Mn}_{2.85}\text{Nb}_{0.15}\text{O}_{10}$  (CMNO),  $\text{Ca}_{0.9}\text{La}_{0.1}\text{MnO}_3$  (CLMO) and  $\text{Ca}_{0.9}\text{Yb}_{0.1}\text{MnO}_3$  (CYMO) compounds, respectively. Starting powders were mixed accordingly to their composition and each compound was thoroughly grinded using an agate mortar and pestle. The samples were heated between 700 and 1150°C for a total period of 48 h with few intermittent grindings. Thus, prepared samples were then cold-pressed in to pellets of 10 mm diameter and sintered again for 12 h.

X-ray diffraction (XRD) patterns were recorded using a bench top X-ray diffractometer (Proto Make AXRD) employing  $\text{CuK}\alpha$  radiation. XRD data of these three compounds were analysed using the PowderX software by assuming orthorhombic unit cell.

For determining thermoelectric properties of these samples, a rectangular slab of the pellet was used. The Seebeck coefficient ( $S$ ) and electrical resistivity ( $\rho$ ) measurements were carried out on Linseis make LSR-3. These quantities were used to calculate the electrical power factor (PF) given as  $S^2/\rho$ .

### 3. Results and discussion

XRD patterns for all the three samples studied during this work are shown along with the Miller indices for the Bragg peaks in figure 2. All the samples have orthorhombic structure. CMNO compound crystallizes in the space group  $Pbca$ , whereas CLMO and CYMO have same structure type and crystallizes in space group  $Pnma$ . The cell parameters were calculated by the least square refinement of the peak positions.

In figure 2, the XRD data clearly shows that all the samples studied here are single phase in nature and their cell parameters are in good agreement with the values reported in the literature [10–12]. For the CLMO and CYMO compounds, it

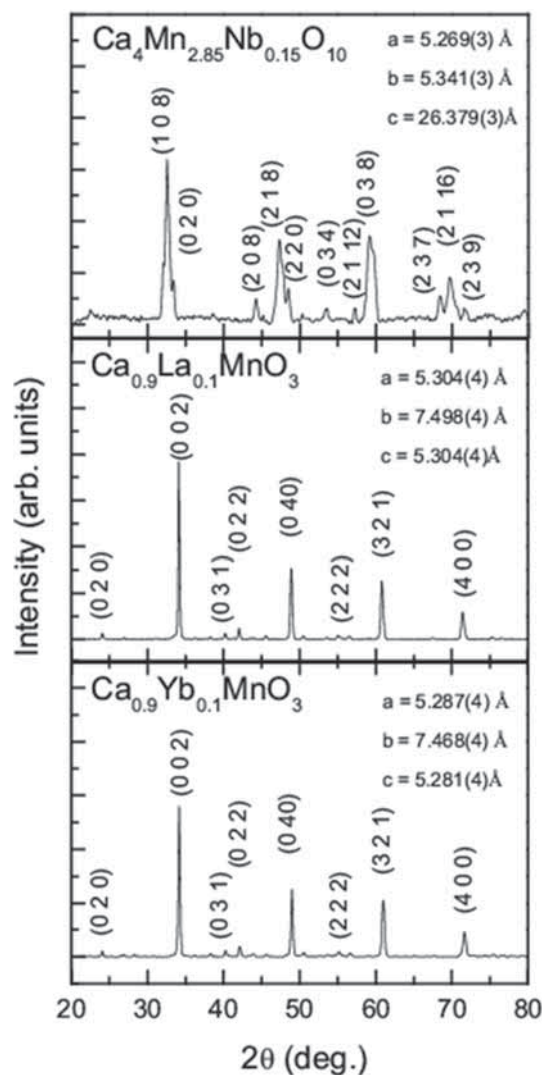


**Figure 2.** XRD patterns for CMNO, CLMO and CYMO samples.

is clearly observed that both the compounds have the same structure type, but by replacing La by Yb, there is reduction in the cell parameters and unit cell volume, which can be attributed to the smaller ionic radii of  $\text{Yb}^{3+}$  ( $\sim 0.868 \text{ \AA}$ ) compared to  $\text{La}^{3+}$  ( $\sim 1.032 \text{ \AA}$ ) [13]. The unit cell volume for CLMO and CYMO is  $\sim 211$  and  $\sim 208 \text{ \AA}^3$ , respectively.

Figure 3 exhibits a plot of electrical resistivity, Seebeck coefficient and power factor, respectively, for CMNO, CLMO and CYMO samples. The data for CMNO sample is plotted on the right axis of each panel. It can be clearly seen from the figure that for CMNO sample, the resistivity ( $\rho = 1/\sigma$ ) is higher than other oxide compounds, whereas the Seebeck coefficient is of the same order, which results in moderate value of power factor ( $\text{PF} = S^2/\rho$ ).

From the literature, it is known that the electronic transport of  $\text{Ca}_4\text{Mn}_3\text{O}_{10}$  shows activated nature due to the hopping of small polarons of dual magnetic-lattice character formed around  $\text{Mn}^{3+}$  impurities left behind due to oxygen sub-stoichiometry [14]. Applying the same analogy to the

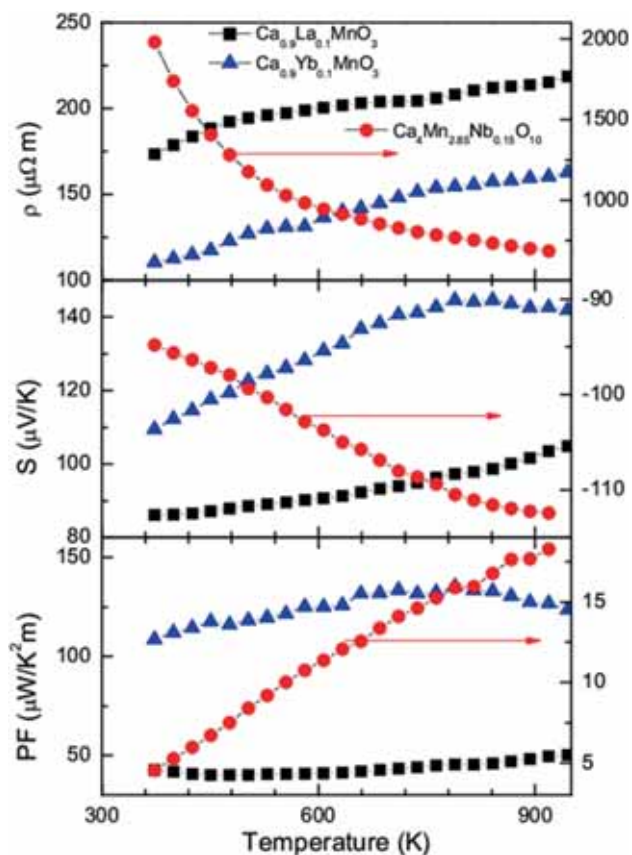


**Figure 3.** Resistivity, Seebeck coefficient and electrical power factor are plotted as a function of temperature for CMNO, CLMO and CYMO samples.

CMNO sample, the higher resistivity can be attributed to the fact that at high temperatures, i.e., in the region of our measurement, the hopping occurs between neighbouring sites, resulting in non-adiabatic transport due to small transfer integral.

The negative sign of Seebeck coefficient for CMNO sample signifies that the majority charge carriers in this compound are *n*-type. Among the two rare-earth-doped  $\text{CaMnO}_3$  compounds, CLMO exhibits higher electrical resistivity compared to CYMO, but the change as a function of temperature is not much, indicating a steady resistance over a large temperature range. In case of Seebeck coefficient also, the order of magnitude of *S* for both the compounds is same, but CYMO exhibits higher values compared to CLMO. Consequently, the PF for CYMO is almost double to that of CLMO. It is an interesting observation, since the only change in both the compounds is the ionic radii, and shrinking of unit cell by about 2%, results in such a drastic change in PF.

#### 4. Conclusion

Comparing PF for *n*- and *p*-type oxides, we observe that there is a good possibility of forming an efficient thermoelectric device using CMNO and CYMO as their performance is appreciable over a wide temperature range. It is desirable to fine-tune PF of CMNO further by an order of magnitude to match that of CYMO for better efficiency.

#### Acknowledgements

APJ would like to thank Technical Physics Division (Bhabha Atomic Research Centre) and Dr K V Sreenivasa Prasad (Prof and Head, Industrial and Production Engineering, SJCE, Mysuru) for providing an opportunity for project internship at BARC. We would also like to acknowledge M Venugopal (UGC-DAE CSR) for the help in sample preparation.

#### References

- [1] Rowe D M 2006 *Int. J. Innovat. Energy Syst. Power* **1** 13
- [2] Walia S, Balendhran S, Nili H, Zhuiykov S, Rosengarten G, Wang Q H *et al* 2013 *Prog. Mater. Sci.* **58** 1443
- [3] Goldsmid J H 2010 *Introduction to thermoelectricity* (New York: Springer) p 1
- [4] Koshibae W and Maekawa S 2008 *Thermoelectric effect in transition metal oxides*, in *Properties and applications: the search for new materials for thermoelectric devices* V Zlatic and A C Hewson (eds). NATO Science for Peace and Security Series B: Physics and Biophysics (The Netherlands: Springer) p 69
- [5] Rowe D M 1996 *CRC handbook of thermoelectrics* (Boca Raton, Boca Raton, FL: CRC Press)
- [6] Roychowdhury S, Panigrahi R, Peruma S and Biswas K 2017 *ACS Energy Lett.* **2** 349
- [7] Banik A, Sandhya Shenoy U, Saha S, Waghmare U V and Biswas K 2016 *J. Am. Chem. Soc.* **138** 13068
- [8] Biswas K, He J, Blum I D, Wu C-I, Hogan T P, Seidman D N *et al* 2012 *Nature* **489** 414
- [9] Ioffe A F *et al* 1956 *Rep. Acad. Sci. USSR* **106** 981
- [10] Chai P, Liu X, Lu M, Wang Z and Meng J 2008 *Chem. Mater.* **20** 1988
- [11] Bhattacharya S, Singh B, Rayaprol S, Singh A, Basu R, Gonal M R *et al* 2011. *AIP Conf. Proc.* **1349** 1011
- [12] Wang Y, Sui Y, Fan H, Wang X, Su Y, Su W *et al* 2009 *Chem. Mater.* **21** 4653
- [13] Shannon R D 1976 *Acta Crystallogr.* **A32** 751
- [14] Lago J, Battle P D, Rosseinsky M J, Coldea A I and Singleton J 2003 *J. Phys. Condens. Matter* **15** 6817